

A DEEP MULTICOLOR SURVEY. III. ADDITIONAL SPECTROSCOPY AND IMPLICATIONS FOR THE NUMBER COUNTS OF FAINT QUASARS

Julia D. Kennefick and Patrick S. Osmer

Astronomy Department, The Ohio State University, 174 West 18th Avenue, Columbus, OH 43210; julia@astronomy.ohio-state.edu and posmer@astronomy.ohio-state.edu

Patrick B. Hall

Steward Observatory, University of Arizona, AZ 85721; phall@as.arizona.edu

Richard F. Green

National Optical Astronomy Observatories, P.O. Box 26732, Tucson, AZ 85726; rgreen@noao.edu

ABSTRACT

We have made spectroscopic identifications of 39 additional quasar candidates from the Deep Multicolor Survey (DMS) of Hall *et al.* (1996, ApJ, 462, 614). We have identified 9 new quasars with $0.3 < z < 2.8$ and $16.8 < B < 21.6$, all from the group of candidates with ultraviolet excess (UVX). No new quasars with $z > 3$ were found among the observed candidates selected due to their red ($B - R$) and ($V - R$) colors. As a result, there are now 55 confirmed quasars in the survey: 42 with $0.3 < z < 2$, nine with $2 < z < 3$, three with $3 < z < 4$, and 1 at $z = 4.3$. One new quasar, DMS 0059–0055, is very bright with $B = 16.8$ and $z = 0.3$, making its detection by our survey very unexpected. Including this new spectroscopy, the results of the DMS are converging with the predicted space densities of other surveys. In particular, we no longer find an excess of quasars with $z < 2.3$ and $B < 21$ in the survey over predictions based on models by Koo & Kron. Also, the excess in the number of quasars seen at $z > 3$ over predictions based on models by Warren, Hewett, & Osmer is less than previously suggested. We also demonstrate the success of our quasar color modeling which is important in assessing the completeness of our survey.

1. Introduction

This is the third in a series of papers describing results from the Deep Multicolor CCD Survey (DMS) of Hall *et al.* (1996ab; Papers I and II) conducted at the KPNO 4m telescope. The survey covered 0.83 deg^2 using six filters (U,B,V,R,I75,I86) covering the range from 0.34 to $0.86 \mu\text{m}$ in six fields at high galactic latitude. The imaging data have average 5σ limiting detection magnitudes ranging from 22.1 to 23.8. The motivation of the survey is to search for lower luminosity quasars at $z > 3$ than have previously been studied and to search for lower luminosity quasars with $z \approx 2$ to constrain the nature of the evolution of the luminosity function. In addition, the survey is valuable for the study of faint field galaxies and stars in the galactic halo (*e.g.*, Liu *et al.* submitted.)

Paper I contains the details of the construction of the stellar catalog of 21375 objects, including a detailed description of the imaging observations and reductions, object classification, photometry, astrometry, and the catalog completeness and contamination. Paper II describes the search for quasars including candidate selection criteria, survey completeness estimates, and initial spectroscopy which resulted in the discovery of 46 quasars, including one at $z = 4.3$, and a comparable number of compact narrow emission line galaxies (CNELG's).

The initial spectroscopy described in Paper II was used along with determinations of the survey efficiency to estimate the number of quasars contained in the survey for different redshift and magnitude bins. Our expected numbers were compared with predictions based on models from Koo & Kron (1988, hereafter KK88) and Warren, Hewett, & Osmer (1994, hereafter WHO). It was concluded that the DMS contains more quasars with $B < 21$ and $z < 2.3$ than expected from the results of Koo & Kron and more quasars at $z > 3$ than expected from the results of Warren, Hewett, & Osmer. However, the initial spectroscopy included less than half of the candidates at the brightest magnitudes and even fewer of the fainter candidates.

Here we report additional follow-up spectroscopy obtained at the KPNO 4m telescope in April and October 1995 resulting in the identification of 39 additional candidates, including the discovery of 9 additional quasars. In §2 we describe the candidate selection process, in §3 we describe the spectroscopic observations and reductions, and in §4 we discuss the spectroscopic results. In §5, we compare our findings with predictions from the determinations of quasar densities from other surveys for quasars. §6 contains further discussion.

2. Candidate Selection

Candidates were selected from the survey catalog of stellar sources as described in Paper II. Briefly, this involves choosing those objects identified as stellar in a majority of the CCD frames that comprise the survey and whose colors are consistent with them being quasars as determined from the colors of simulated quasar spectra.

In all, 51 previously unidentified candidates were observed. Twenty-four were bright ultraviolet

excess (UVX) objects ($16.5 < B < 21.0$) and 13 were fainter UVX objects ($21.0 < B < 22.0$). These candidates are expected to have $z < 3$. Candidates for $z > 3$ quasars included 5 objects selected as outliers according to their UBVR magnitudes (VRX) and nine objects with very red ($B - R$) colors (BRX).

For longslit observations with Cryocam on the KPNO 4m in April 1995, we used the selection criteria outlined in Paper II to select targets in the 10h field (which had not been previously investigated spectroscopically), targets previously observed but with inconclusive spectra, bright targets requiring only brief exposures, and most of the remaining VRX and BRX candidates accessible in the northern spring (most such remaining candidates are fall objects). Where possible, the slit was rotated and placed so that any other candidates located within about $2'$ of the primary candidates, and of similar magnitude, could be observed simultaneously. Typically these were UVX candidates, as they are the most common. In fields with no secondary candidate the slit was oriented to observe a galaxy within $2'$ chosen by C. Liu to calibrate photometric redshifts calculated for galaxies in these fields (Liu *et al.* submitted).

The primary targets for our October 1995 KPNO 4m run were the BRX and VRX candidates for which no spectra, or inadequate spectra, existed. Since most of these are faint and would require long integrations, we created multislit masks so that as before, secondary candidates and/or nearby galaxies could be observed simultaneously whenever possible. Unfortunately the Cryocam CCD was not functioning at this time and the lower-efficiency RC Spectrograph was used, requiring longer integration times and preventing us from identifying the faintest candidates.

3. Spectroscopic Observations and Reductions

3.1. April 1995

We used the Cryocam on the KPNO 4m telescope on UT 1995 April 22-24 to take spectra of observable candidates. Candidates were chosen for spectroscopy as outlined in §2. Conditions were clear with poor seeing.

A Loral 800 x 1200 CCD, formatted to 471 x 1200, was used with a gain of 1.5 electrons/ADU. We chose grism #770 (300 lines/mm) and a blocking filter with a blue cutoff at 3850\AA . This gives a dispersion of $4.3\text{\AA}/\text{pixel}$ and wavelength coverage from 4500 to 8500\AA . We used a single slit of $1.7''$ giving a resolution of 15\AA . Object exposures ranged from 600s to 2100s, with the most common exposure time being 1800s.

The raw two-dimensional CCD frames were corrected for overscan and bias using the IRAF¹ CCDRED package. Pixel-to-pixel variations were corrected using a quartz flat field normalized

¹The Image Reduction and Analysis Facility (IRAF) is distributed by the National Optical Astronomy Observatories, which is operated by AURA, Inc., under contract to the National Science Foundation.

using the IRAF RESPONSE routine to remove the wavelength dependence of the flat that is mainly due to the lamp. The spectra were then extracted and wavelength and flux calibrated using the IRAF DOSLIT package with HeNeAr comparison frames and standard star observations that were obtained each night.

3.2. October 1995

As the Cryocam was not available, we used the RC Spectrograph on UT 1995 October 27-29 to take spectra of candidates chosen from our fall fields. Conditions were generally good with some cirrus on the last night. Multislit masks were used so that spectra of secondary candidates could be obtained during the long exposures needed to detect faint candidates.

A Tektronix 2048² CCD formatted to 2048 x 651 was used with a gain of 2.0 electrons/ADU. We chose grating BL181 (316 lines/mm) and blocking filter GG455 giving a dispersion of 2.8Å/pixel and wavelength coverage of 4100Å ranging from 4600Å to 10000Å depending on the particular mask and slit position. The slitmasks had 2.5'' slit widths giving a resolution of 10Å. Object exposures ranged from 1200s to 2400s.

For each object mask, typically two object exposures were taken and combined before extraction. Quartz flats and HeNeAr comparison frames were taken between the two object exposures at the same telescope position. Brighter candidates were observed with single shorter exposures in one slit of a multislit mask or with a single long slit mask, also of 2.5'' width. Quartz flats and comparisons were obtained for these exposures immediately before or after the observation at the same telescope position.

The two-dimensional CCD frames were corrected for overscan and bias using the IRAF CCDRED package. For multislit masks or those objects observed through a single aperture of a multislit mask, the images were corrected for pixel-to-pixel variations using flat fields created from the quartz lamp images using the IRAF APFLATTEN routine which removes the wavelength structure introduced by the quartz lamp. The spectra were then extracted and wavelength calibrated using the TWODSPEC package in IRAF. For those objects observed through the long slit mask, pixel-to-pixel variations were removed using a quartz flat field obtained at the same pointing as the object frame normalized using the IRAF RESPONSE routine. The spectra were then extracted and wavelength calibrated using the IRAF DOSLIT package. The spectra were not flux calibrated.

4. Spectroscopic Results

A total of 57 candidates were observed in April and October, 1995. Of these, six were objects previously identified as quasars, but with some doubt because the spectra were of low S/N. All

six were again identified as quasars. Spectroscopy was repeated for nine candidates that were observed previously but that could not be identified. Six of these were identified from this new spectroscopy, four as galaxies, one as a CNELG, and one as a star. Three others still could not be identified due to the poor S/N level of the data. In total, 39 new candidates were identified: nine quasars, 4 CNELG’s, 8 galaxies, and 18 stars. Twelve other candidates were observed but could not be identified.

4.1. Quasars

The list of the nine new quasars found from this spectroscopy is given in Table 1 including positions, magnitudes, redshifts, and notes. The objects are numbered following on from Table 1 of Paper II. All of these quasars were chosen as UVX candidates. Their redshifts span the range $0.296 < z < 2.80$ and their magnitudes $16.8 < B < 21.6$. This brings the total number of quasars found by the DMS survey to date to 55 spanning the redshift range $0.296 < z < 4.33$. There are 42 objects with $z < 2$, nine with $2 < z < 3$, three with $3 < z < 4$, and one at $z = 4.33$.

Five of the nine quasars reported here have been identified as quasars on the basis of the presence of one broad emission line in their spectrum. In all cases, this line has been identified as Mg II on the basis of its profile and the absence of other emission lines. The other four quasars were assigned redshifts on the basis of at least 2 broad emission lines. Of note is DMS 0059–0055, the brightest and lowest redshift quasar found in this survey to date with $z = 0.296$ and $B = 16.8$. Its spectrum, shown in Figure 1, shows prominent Fe II emission. At $z = 0.296$ and $B = 16.8$, it has $M_B = -23.66$ (for $H_0 = 75 \text{ kms}^{-1} \text{ Mpc}^{-1}$, $q_0 = 0.5$, and assuming a spectral index of $\alpha = -0.75$), making it a *bona fide* quasar. None of the BRX or VRX candidates observed in 1995 were identified as quasars.

4.2. Compact Narrow Emission Line Galaxies

Four of the candidates were identified as compact narrow emission line galaxies (CNELG’s) at redshifts $0.40 < z < 0.66$. Table 2 lists their positions, B magnitudes, redshifts, and notes on the objects. The objects are numbered following on from Table 2 of Paper II. All of the objects have weak narrow lines. As mentioned in Paper II, CNELG’s can be a major source of contamination in UVX surveys for quasars (see Paper II, Figure 9.) In the initial spectroscopy reported in Paper II, almost as many CNELG’s were recovered as quasars at $z < 3$. Subsequently, an additional requirement of $(B - V) < 0.60$ was adopted in candidate selection to improve the discrimination between quasars and CNELG’s. The ratio of CNELG’s to UVX quasars recovered from the spectroscopy reported here is $\sim 44\%$, much lower than that reported in Paper II. Thus this additional requirement has eliminated a substantial fraction of these objects, as intended.

5. Surface Densities

From the initial spectroscopy, together with the extensive modeling and simulations presented in Paper II, we estimated that the survey contained more quasars with $B < 21$ and $z < 2.3$ than expected from the KK88 survey and more quasars with $z > 3$ than expected from the results of WHO. We have recomputed estimated numbers of quasars contained in the DMS based on our new spectroscopic data (Tables 3A, 3B, and 4). The methods used are the same as those given in Paper II. Briefly, predicted quasar counts are computed by multiplying the number of candidate objects we have selected using a given method by the observational efficiency for that method (the number of confirmed quasars divided by the number of spectroscopic IDs). The expected number of quasars as predicted by previous surveys is computed by numerically integrating the QLF determined by the survey over the redshift and magnitude ranges of interest including the detection probabilities of the DMS survey as a function of redshift and magnitude as reported in Paper II.

5.1. $z < 3$: The UVX Objects

Observed and expected numbers of UVX quasars in the DMS are given for different B magnitude bins at $z < 2.3$ (Table 3A) and $z > 2.3$ (Table 3B.) The number of candidates in each magnitude bin is listed along with the number of spectroscopic identifications, the number of confirmed quasars, the resulting observational efficiency, and the estimated number of quasars that are contained in the survey. The 1σ confidence limits are given using the method tabulated by Gehrels (1986) for small numbers of events². We have recomputed the expected number of quasars using the results of KK88 and also show the expected number based on the results of Boyle *et al.* (1988, hereafter BSP).

Previously we had computed an observational efficiency of 50% at $z < 2.3$ and $B < 21$. Adding our new spectroscopy, this drops to 39.0% and decreases the estimated number of quasars from 41.5 to 32.4. This result is in good agreement at the 1σ level with both KK88 and BSP who predict 29.6 and 32.7, respectively. Based on the new spectroscopy and our updated computation of the number of expected quasars from KK88, we see no evidence for an excess of quasars in our survey at $z < 2.3$ and $B < 21$. At $z > 2.3$ and $B < 21$, our results agree with those of BSP at the 1σ level and agree with KK88 at the 2σ level. We have now identified over 70% of the $B < 21$ UVX candidates.

Given the decline in the observational efficiencies in this magnitude bin compared with Paper II, one may wonder if they are likely to decrease even more as the remaining candidates are observed, thus resulting in lower predicted numbers of quasars. However, the remaining candidates

²Some 1σ errors presented in Tables 3 and 4 of Paper II were incorrect due to a small computational error.

do not occupy regions of color-color space different from those occupied by the candidates already observed. Therefore, we do not expect observational efficiencies to be significantly different for our remaining candidates. One issue that was mentioned in Paper II and that remains a factor here is that proportionally fewer candidates at $(U - B) > -0.3$, where quasars at $z > 2.3$ are expected, have been observed than at $(U - B) < -0.3$, where quasars at $z < 2.3$ are expected (60% *vs.* 80% for $B < 21.0$.) If we compute observational efficiencies for these two areas separately, we predict 28.4 quasars at $z < 2.3$ (instead of 32.4) and 6.2 quasars at $z > 2.3$ (instead of 5.6.) However, this is still in good agreement with both KK88 and BSP.

Estimated and predicted numbers of UVX quasars in the range $21 < B < 22$ are in good agreement at the 1σ level at $z > 2.3$ and at the 2σ level at $z < 2.3$ for both KK88 and BSP and have not changed significantly since Paper II. For UVX quasars at $B > 22$ we have not completed enough spectroscopy to give statistically significant results, but given our average observational efficiency of $\sim 35\%$ at $z < 2.3$, we are selecting numbers of candidates roughly consistent with the results of KK88 and BSP.

5.2. $z > 3$: The VRX and BRX Objects

Table 4 lists observed *vs.* predicted numbers of VRX and BRX quasars at $z > 3$. Given is the number of candidates chosen from each method, the number of candidates for which spectroscopy has been obtained, the number of confirmed $z > 3$ quasars, the observational efficiency, the resulting estimated number of $z > 3$ quasars contained in the survey, and expected numbers of quasars as predicted by two surveys for quasars at high redshift. Some $z > 3$ quasars were selected both as VRX and BRX objects. Of the 12 candidates observed in 1995 but that remain unidentified, eight are UVX candidates and four are BRX candidates. While it is possible that the unidentified UVX objects are quasars at $z < 3$ whose redshifts are such that no strong lines are in the wavelength range covered by the spectroscopy, it is unlikely that the unidentified BRX objects are quasars at $z > 3$, as the Lyman α line and the drop blueward of the line produce a strong, distinct feature and should have been detectable in our spectra. Therefore observational efficiencies were computed by dividing the number of confirmed quasars by the number of candidates that have been observed spectroscopically even if the candidate could not be assigned a firm identification.

The expected numbers of quasars were computed by integrating the QLF of WHO from $z = 3$ to 5 over the magnitude range of interest and including DMS detection probabilities. The last column of Table 4 contains the number of quasars expected from computing quasar counts as outlined in Kenefick *et al.* (1995, hereafter KDC). This involves scaling the Boyle *et al.* (1988) $z = 2$ QLF down in density by 6.5 to match the results of Schmidt *et al.* (1995, hereafter SSG) and KDC at $z = 4.4$ and adopting the evolution predicted by SSG, that is, that quasar space densities fall off by a factor of 2.7 per unit redshift beyond $z = 2.7$.

The WHO survey predicts approximately twice as many quasars as does KDC for the VRX method. This is because the evolution adopted by KDC is taken from SSG who predict that quasar space densities begin to decline at $z = 2.7$ while WHO find a peak at $z = 3.3$ and a decline beyond. The DMS VRX detection probabilities (Paper II, Figure 16) are high at $z = 3.0$ to 3.5 where the WHO space densities are peaking, resulting in higher expected numbers. The DMS survey finds one quasar at $V < 20.5$ while the WHO and KDC surveys predict 2.4 and 1.5 respectively. At $20.5 < V < 22.0$, the DMS survey estimates three quasars at $z > 3$ while WHO and KDC find 3.8 and 1.9 respectively. These numbers seem to be in good agreement although the numbers involved are small, making any conclusions tentative.

Here, we have combined the four different magnitude bins for the BRX method from Paper II in to one bin at $17.5 < R < 22.0$. The DMS has found three confirmed quasars from the 21 observed BRX candidates. This leads us to predict that the survey contains one additional quasar in the seven candidates that we have yet to observe for a total of four. This is down from an estimated number of 8.4 from Paper II. Observational efficiencies have dropped from 30% to 14%. However, the color-color space has now been well explored and the remaining candidates do not occupy regions of the space different from those already investigated, so we do not expect this observational efficiency to change significantly as the remaining candidates are observed.

The number of expected quasars is higher for KDC than for WHO in the BRX case because while DMS BRX detection probabilities are rising steeply beyond $z = 3.5$ to over 95% at $z > 3.8$, WHO predicts that space densities are dropping much more steeply as a function of redshift than predicted by SSG. WHO predict 1.2 quasars while KDC predict 2.0. While we still find that the DMS contains an excess of objects at $z > 3$ over that expected from the results of WHO and KDC, it is only at the $2 - 3\sigma$ level, and, given the small number of objects at $z > 3$ contained in the DMS and that the WHO and KDC results themselves are based on a relatively small number of objects, we do not find the excess statistically significant. On the other hand, it could indicate that the decline in quasar space densities at high redshift is too steep in both the WHO and SSG cases. Also, we can't rule out the possibility that there is luminosity-dependent evolution in the QLF and that the results of both WHO and SSG cannot be extrapolated to the fainter magnitudes of the DMS.

6. Discussion

Multicolor surveys can suffer from large selection biases that vary with redshift, magnitude, and spectral energy distribution (SED.) We have attempted to model these biases by producing synthetic quasar spectra with a variety of properties (see Paper II, §5 for a detailed description of the synthetic spectra) and determining the probability of selecting such quasars given our candidate selection procedures. The question then arises: are the models actually representative of the data? Figure 2 demonstrates that the theoretical quasar colors computed from the synthetic spectra do accurately model the colors of the quasars contained in the DMS. Shown is a $(B - V)$

vs. $(U - B)$ color-color diagram containing the 27 UVX quasars in the range $(16.5 < B < 21.0)$ along with their redshifts. Theoretical quasar colors computed from the synthetic spectra are plotted as tracks. Four different quasar SED are shown with varying line strengths and spectral slopes (α) and with redshifts ranging from $z = 0.05$ to 3.05 in steps of 0.1 . The theoretical tracks do bracket the survey quasar colors and the trend in color with redshift is also matched quite well. In particular, note the two quasars at $z \approx 2.8$ at $(B - V) \approx 0.3$ and $(U - B) \approx 0$. They would have been predicted to be in the redshift range between $z = 2.4$ and 2.9 based on their colors alone. Since the synthetic quasar spectra play a major role in computing the survey completeness, the good agreement between their colors and those of the real quasars lends more confidence in our results.

The discovery of the one bright quasar at $z = 0.296$ and $B = 16.8$ and the quasar at $z = 4.3$ and $R = 20.1$ are unexpected in 0.83 deg^2 , the area of the DMS survey. We could expect to find 0.04 quasars at $z < 2.2$ and $16.5 < B < 17.0$ in the DMS based on the QLF of Boyle *et al.* (1988), or one every 28 deg^2 . The Large Bright Quasar survey of Hewett *et al.* (1995) found 15 quasars with $16.5 < B < 17.0$ in an effective area of 454 deg^2 , or one every 30 deg^2 . The Hamburg/ESO Survey (Köhler *et al.* 1997) and the Homogeneous Bright QSO Survey (La Franca & Cristiani 1997) also predict one such quasar every $\sim 30 \text{ deg}^2$. Given the agreement of these surveys at these magnitudes, it was indeed unlikely that this bright object would be found in the DMS. As for the $z = 4.3$ quasar, we could expect to find 0.06 quasars at $4.0 < z < 4.5$ and $19.5 < R < 20.5$ in the DMS based on the results of WHO or 0.28 based on the results of KDC, or one quasar every 13 or 3 deg^2 , respectively. While these results are unexpected, due to their small numbers, we do not find their discovery statistically significant.

The spectroscopy reported here brings the total number of quasars in the DMS to 55 , four of these having $z > 3$. Given our observational efficiencies including this new spectroscopy, we conclude that the number of quasars estimated to be contained in the DMS is in good agreement with the results of other surveys for quasars. The absence of new quasars with $z > 3$ among the BRX candidates reduces the expected total number of such quasars in the survey from 8.4 to 4.0 . This is not a significant excess over the predicted number of 1.2 (allowing for efficiency of detection) based on results by WHO or of 2.0 based on results by KDC, and, therefore, the estimated number of objects in the DMS at $z > 3$ are in good agreement with these two surveys. The results for the UVX candidates indicate that the number of quasars in the survey with $z < 2.3$ and $B < 22$ is also less than estimated in Paper II and in good agreement with the predictions of the KK88 and BSP surveys.

Unfortunately, we were unable to identify any additional UVX candidates at $B > 22.0$ beyond what was reported in Paper II. This spectroscopy along with that of the remaining BRX candidates will require an instrument/telescope combination with greater sensitivity than the configurations used here.

The next steps are to complete the spectroscopy of the BRX candidates so that a definitive

value of the surface density of faint $z > 3$ quasars in the survey is established; complete the spectroscopy of the UVX candidates with $B > 22$ to constrain the evolution of the faint end of the luminosity function at $z < 2.3$; make the entire catalog available to the community in electronic form; and identify and analyze the field galaxies and faint stars.

We would like to thank the KPNO mountain staff for their assistance in observing and the KPNO TAC for their allocation of time for this project. We also thank an anonymous referee for useful comments. This work was supported in part by NSF Award AST-9529324.

REFERENCES

- Boyle, B.J., Shanks, T., and Peterson, B.A. 1988, MNRAS, 235, 935 (BSP)
- Gehrels, N. 1986, ApJ, 303, 336
- Hall, P.B., Osmer, P.S., Green, R.F., Porter, A.C., and Warren, S.J. 1996a, ApJS, 104, 185 (Paper I)
- Hall, P.B., Osmer, P.S., Green, R.F., Porter, A.C., and Warren, S.J. 1996b, ApJ, 462, 614 (Paper II)
- Hewett, P.C., Foltz, C.B., and Chaffee, F.H. 1995, AJ, 109, 1498
- Kennefick, J.D., Djorgovski, S.G., and de Carvalho, R.R. 1995, AJ, 110, 2553 (KDC)
- Köhler, T., Groote, D., Reimers, D., and Wisotzki, L. 1997, A&A, in press
- Koo, D.C. and Kron, R.G. 1988, ApJ, 325, 92 (KK88)
- La Franca, F. and Cristiani, S. 1997, AJ, submitted
- Liu, C.T., Green, R.F., Hall, P.B., and Osmer, P.S. 1997, AJ, submitted
- Schmidt, M., Schneider, D.P., and Gunn, J.E. 1995, AJ, 110, 68 (SSG)
- Warren, S.J., Hewett, P.C., and Osmer, P.S. 1994, ApJ, 421, 412 (WHO)
- Wilkes, B.J. 1986, MNRAS, 218, 331

Table 1. Quasars: Identifications

Number ^a	I.D.	R.A.(1950)	Dec.(1950)	<i>B</i> mag	<i>z</i>	Notes
47	DMS 0059–0104	00 ^h 59 ^m 38 ^s .38	–01°04′19″.80	21.6	1.05?	one line, Mg II?
48	DMS 0059–0055	00 59 52.82	–00 55 10.73	16.8	0.296	strong lines
49	DMS 1034–0040	10 34 33.91	–00 40 59.68	18.6	1.22?	one line, Mg II?
50	DMS 1034–0045	10 34 39.13	–00 45 27.26	19.7	0.94?	one line, Mg II?
51	DMS 1358–0101	13 58 18.34	–01 01 55.16	21.5	1.25?	one line, Mg II?
52	DMS 1358–0052	13 58 22.70	–00 52 18.89	20.4	0.85?	one line, Mg II?
53	DMS 1358–0102	13 58 29.92	–01 02 41.64	20.1	0.82	Mg II, H γ
54	DMS 1714+5012	17 14 21.08	+50 12 33.86	20.1	2.80	Ly α , C IV
55	DMS 1714+5021	17 14 51.80	+50 21 12.67	21.1	1.51	C III], Mg II

^aThe numbers follow on from Table 1 of Paper II

Table 2. Compact Narrow Emission-Line Galaxies: Identifications

Number ^a	I.D.	R.A.(1950)	Dec.(1950)	<i>B</i> mag	<i>z</i>	Notes
40	N0100–0101	01 ^h 00 ^m 32 ^s .11	–01°01′12″.28	23.9	0.67	weak lines
41	N1034–0043	10 34 01.57	–00 43 40.07	21.8	0.66	weak lines
42	N1358–0059	13 58 08.90	–00 59 48.55	21.9	0.400	weak lines
43	N2245–0214	22 45 46.33	–02 14 26.50	20.8	0.425	weak lines

^aThe numbers follow on from Table 2 of Paper II

Table 3a. Observed versus Predicted Numbers of $z < 2.3$ UVX Quasars

Magnitude Bin Limits	No. of UVX Candidates	No. of UVX ID's	Confirmed $z < 2.3$ Quasars	Observational Efficiency	Estimated Number of $z < 2.3$ Quasars	Expected No. of $z < 2.3$ Quasars ^a	
						KK88	BSP
$16.5 < B < 21.0$	83	59	23	$39.0^{+7.3}_{-6.9}\%$	$32.4^{+3.0}_{-2.9}$	29.6	32.7
$21.0 < B < 22.0$	71	33	17	$51.5^{+10.0}_{-10.1}$	36.6 ± 4.9	41.8	31.0
$22.0 < B < 22.6$	99	10	2	$20.0^{+20.7}_{-12.8}$	$19.8^{+18.8}_{-12.0}$	48.2	26.0
$22.6 < B < 23.1$	145	0	0	42.8	18.4

^aCalculated by convolving the number-magnitude relation of Koo & Kron 1988 (KK88) and the luminosity function of Boyle, Shanks, & Peterson 1988 (BSP) with the UVX detection probabilities as discussed in the text.

Table 3b. Observed versus Predicted Numbers of $z > 2.3$ UVX Quasars

Magnitude Bin Limits	No. of UVX Candidates	No. of UVX ID's	Confirmed $z > 2.3$ Quasars	Observational Efficiency	Estimated Number of $z > 2.3$ Quasars	Expected No. of $z > 2.3$ Quasars ^a	
						KK88	BPS
$16.5 < B < 21.0$	83	59	4	$6.8^{+5.1}_{-3.2}\%$	$5.6^{+1.7}_{-1.5}$	3.4	4.4
$21.0 < B < 22.0$	71	33	1	$3.0^{+6.9}_{-2.4}$	$2.2^{+2.8}_{-1.4}$	3.6	3.8
$22.0 < B < 22.6$	99	10	0	$0.0^{+16.8}_{-0.0}$	$0.0^{+15.0}_{-0.0}$	3.3	2.3
$22.6 < B < 23.1$	145	0	0	1.4	0.9

^aCalculated by convolving the number-magnitude relation of Koo & Kron 1988 (KK88) and the luminosity function of Boyle, Shanks, & Peterson 1988 (BSP) with the UVX detection probabilities as discussed in the text.

Table 4. Observed versus Predicted Numbers of VRX and BRX Quasars

Selection Method	Magnitude Bin Limits	No. of Candidates	No. of Spectra	Confirmed $z > 3$ Quasars	Observational Efficiency	Estimated Number of $z > 3$ Quasars	Expected Number of $z > 3$ Quasars	
							WHO ^c	KDC ^d
VRX ^a	$17.5 < V < 20.5$	3	3	1	$33.3^{+41.5}_{-26.7}\%$	1.0 ± 0.0	2.4	1.5
VRX ^a	$20.5 < V < 22.0$	3	2	2	100 ± 0.0	$3.0^{+0.0}_{-1.0}$	3.8	1.9
BRX ^b	$17.5 < R < 22.0$	28	21	3	$14.3^{+12.1}_{-7.7}$	$4.0^{+1.3}_{-1.1}$	1.2	2.0

^aBased on $(U - V)/(V - R) + (B - V)/(V - R)$ color-color diagrams

^bBased on $(B - R)/(R - I86) + (B - R)/(I75 - I86)$ color-color diagrams

^cCalculated using the luminosity function of Warren, Hewett, & Osmer 1994 (WHO) and the survey detection probabilities.

^dCalculated using the survey detection probabilities and the luminosity function of Boyle, Shanks, and Peterson 1988 scaled to the results of Kenefick *et al.* 1995 (KDC) and Schmidt, Schneider, & Gunn 1995 (SSG) at $z \sim 4$ and adopting the SSG form of evolution in quasar space densities.

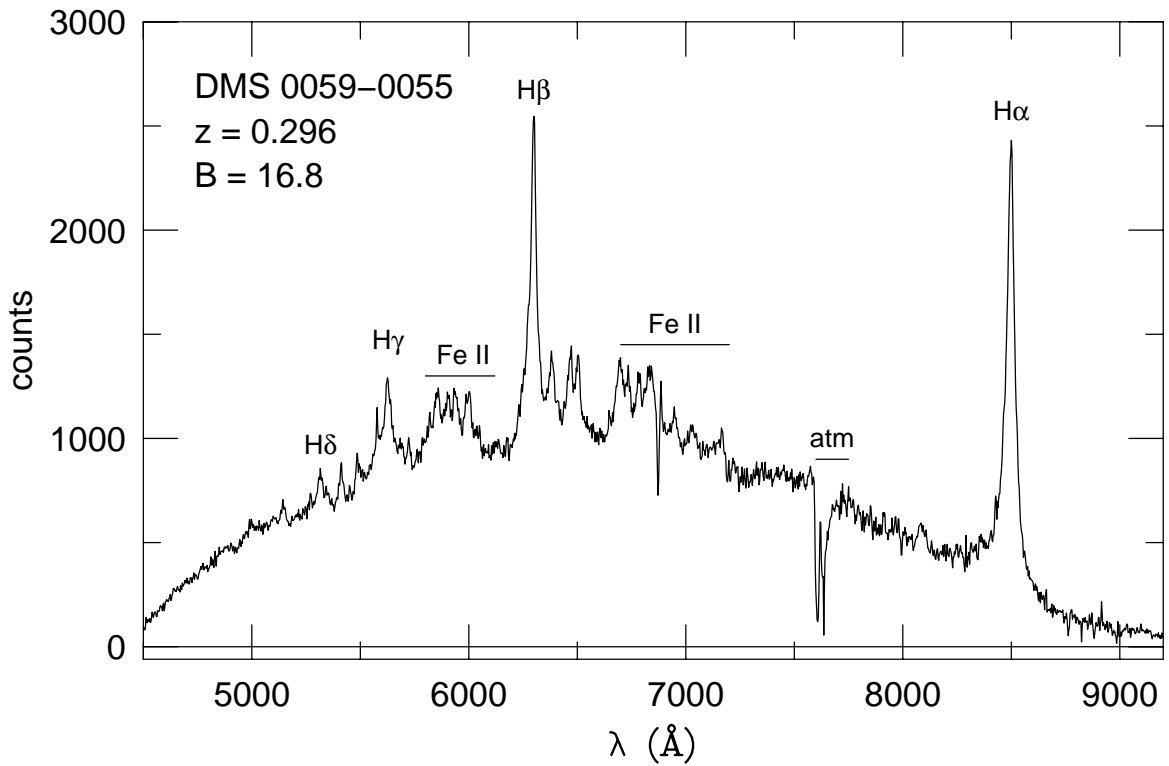


Fig. 1.— A spectrum of DMS 0059–0055, a bright quasar at $z = 0.296$. The 900 second spectrum was obtained with the RC Spectrograph at the KPNO 4 meter telescope on UT 1995 October 28. This is the brightest and lowest redshift quasar in the survey.

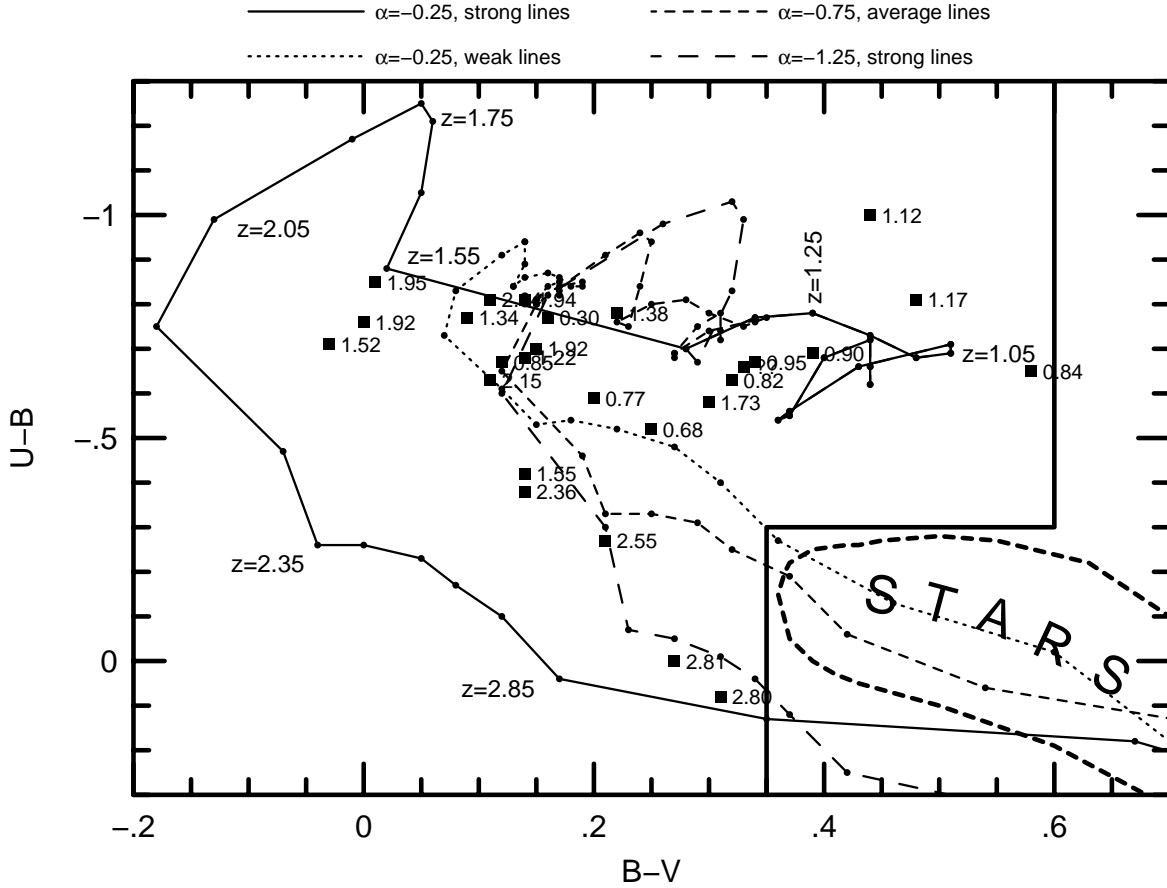


Fig. 2.— A $(B - V)$ vs. $(U - B)$ color-color diagram showing the 27 UVX survey quasars in the range $(16.5 < B < 21.0)$ (filled squares). The redshift of the quasar is given to the right of the symbol. Also shown are the candidate selection limits (heavy solid line) and the approximate location of the stellar locus. Theoretical color-redshift tracks are also shown for a variety of quasar continuum slopes (α) and emission line strengths as indicated above the diagram. Average line strengths were taken from Wilkes (1986) with weak lines taken as half the equivalent width of average lines and strong lines taken as twice the equivalent width. The tracks as shown cover the redshift range from 0.05 to 3.05 in steps of 0.1 (dots). The redshift of a few points is indicated for one track (solid line, $\alpha = -0.25$, strong emission lines) and should allow the reader to infer the redshifts for points on the other tracks based on the shape of the tracks. For further discussion, see §6.